

# *p-n* Junctions in Bulk and Two-Dimensional Materials

Kraig Andrews\*

Wayne State University Department of Physics and Astronomy

(Dated: December 12, 2017)

## I. INTRODUCTION TO *p-n* JUNCTION

A *p-n* junction is formed when a *p*-type semiconductor is and an *n*-type semiconductor are in contact. Understanding this basic configuration creates a foundation for much of modern electronic applications and other semiconductor devices. These *p-n* junctions are fundamental to a variety of functions such as rectification, amplification, switching, and other applications which can be achieved by varying parameters of the junction.

## II. *p-n* JUNCTION IN EQUILIBRIUM

In the most basic sense, one can consider a *p-n* junction under thermodynamic equilibrium with constant doping concentrations. The band diagrams of the *p* and *n*-type materials before they are brought into contact with each other are pictured in fig. 1. Once the regions of differ-

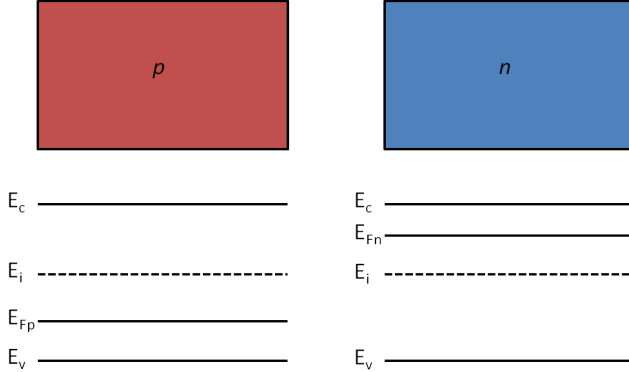


FIG. 1: Energy band diagram of the *p* and *n*-type regions taken separately.

ing types are brought into contact with each other the band diagram is as pictured in fig. 2. Once the two material types are connected and the Fermi levels are aligned then the electrons diffuse from the electron-rich *n*-type (*p*-type) material to the electron-lacking (hole-lacking) *p*-type (*n*-type) region. The diffusion of charges across the junction creates an internal built-in potential denoted by  $\Phi_0$  in fig. 2 and in equilibrium is dependent upon the thermal voltage, doping concentrations, and intrinsic carrier concentration of the semiconductor. The

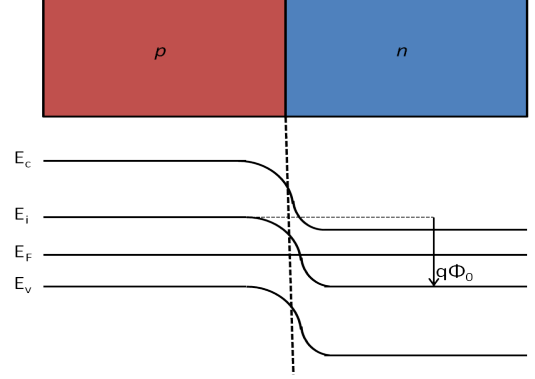


FIG. 2: Energy band diagram of a *p-n* junction.

built-in potential is given by

$$\Phi_0 = \frac{k_B T}{q} \ln \left( \frac{N_a N_d}{n_i^2} \right), \quad (1)$$

where the term  $k_B T/q$  is the thermal voltage  $V_T$ ,  $N_a$  and  $N_d$  are the acceptor and donor doping concentrations, respectively, and  $n_i$  is the intrinsic carrier concentration of the semiconductor. When the electrons (holes) diffuse from the *n*-type (*p*-type) region into the *p*-type (*n*-type) region ionized donor (acceptor) atoms are left in their place. This creates a depletion region on each side of the junction as shown in fig. 3 where  $W_p$  and  $W_n$  denotes the depletion region widths on the *p* and *n* sides, respectively and can be expressed as

$$W_{V_a=0} = \sqrt{\frac{2\epsilon \Phi_0 (N_a + N_d)}{q N_a N_d}}. \quad (2)$$

In the case of an abrupt *p-n* junction, one that can be

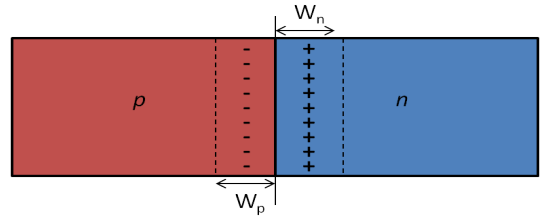


FIG. 3: Depletion region width depiction on both the *n*-side and *p*-side,  $W_n$  and  $W_p$ , respectively.

modeled as step-function at the transition from the depletion region to the charge-neutral *p* and *n*-type regions, there are two boundary conditions that must be satisfied.

\* kraig.andrews@wayne.edu

First, that at the boundary of the depletion region, the electric field must go to zero. Written in a mathematical form this implies that

$$E(x = W_{p,n}) = 0. \quad (3)$$

Second, we define the point  $x = 0$  to be the transition within the depletion region from the  $p$ -type to the  $n$ -type regions, at this point, the electric field must be continuous. This condition written more compactly can be expressed as

$$E(x = \delta_p) = E(x = \delta_n), \quad (4)$$

where  $\delta_p$  and  $\delta_n$  are some infinitesimally small distance on the  $p$  and  $n$ -side, respectively. Together, these two conditions can be used to solve the Poisson equation and give a mathematical description of  $p$ - $n$  junction.

### III. $p$ - $n$ JUNCTION IN NON-EQUILIBRIUM

Previously, the  $p$ - $n$  junction has been discussed when in equilibrium, when  $V_a = 0$ . However, when the configuration is no longer in equilibrium, when a bias voltage is applied, the details of the junction change. Fig. 4 shows the energy band diagram of the junction under both reverse bias ( $V_a < 0$ ) and forward bias ( $V_a > 0$ ). In each case, there are a number of effects that result. First, under reverse bias, the built-in potential is effectively increased. In addition, the depletion region width increases as the depletion region width can be described as

$$W_{V_a \neq 0} = \sqrt{\frac{2\epsilon (\Phi_0 - V_a) (N_a + N_d)}{q N_a N_d}}. \quad (5)$$

Fig. 5 shows the depletion region under reverse bias in which the increase in the depletion width can be clearly seen. Another effect seen under reverse bias is that the diffusion of hole in the  $n$ -type region and diffusion of electrons in the  $p$ -type region are reduced and the net current, resulting from the drift of holes from the  $n$ -type region into the  $p$ -type region and the drift of electrons from the  $p$ -type region into the  $n$ -type region is observed. Conversely, under forward bias the built-in potential is effectively reduced and the depletion region is also decreased in width. Also, in contrast with the reverse bias regime, under forward bias there is increased diffusion current because the potential is reduced so that the electric field and diffusion are no longer equal and opposite. This is because the diffusion force acting on the carriers is only partially compensated for by the force resulting from the junction potential variation and therefore, holes can flow from the  $p$ -type region into the  $n$ -type semiconductor and electrons can flow from the  $n$ -type region into the  $p$ -type semiconductor [4].

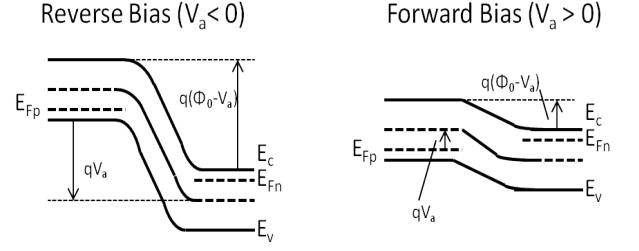


FIG. 4: Energy band diagram on  $p$ - $n$  junction at forward and reverse bias.

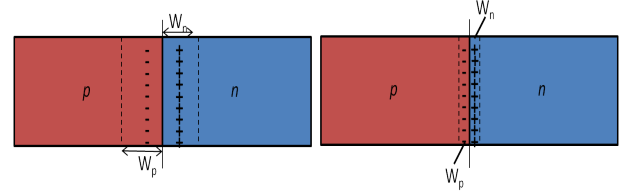


FIG. 5: Depletion region changes under reverse and forward bias

### IV. CURRENT-VOLTAGE CHARACTERISTICS

Thus far ideal  $p$ - $n$  junctions have been discussed and several assumptions have been made to make this possible. First, an abrupt depletion layer has been assumed. This implies that the built-in potential and applied voltages are supported by a dipole layer with abrupt boundaries, and outside the boundaries the semiconductor is assumed to be charge neutral. Second, the Boltzmann approximation has been assumed to be valid. Meaning that the semiconductor doping level are non-degenerate. If this is not the case then Fermi-Dirac statistics must be employed. Third, it has been assumed that the injected minority carrier densities are small compared to the major carrier densities. If this is not the case, then the high-injection regime has been entered. This will be discussed in more detail in the next section. Lastly, it is assumed that there is no generation or recombination current present inside the depletion layer, and the electron and hole currents are constant throughout the depletion layer. Taking these four assumptions into account, then the ideal current-voltage characteristics are presented in fig. 6. Note that the minority carriers are small compared to the majority carriers on each side. The hole current density  $J_p$  is large compared to the electron carrier density  $J_n$  on the  $p$ -side and the electron carrier density is large compared to the hole carrier density on the  $n$ -side. In addition, throughout the depletion region both  $J_p$  and  $J_n$  are constant in both forward and reverse bias [4].

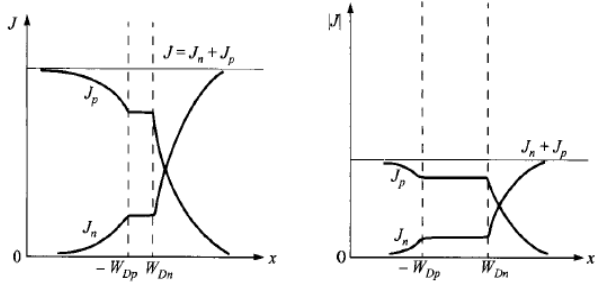


FIG. 6: Shockley current density as a function of position within the semiconductor structure at forward and reverse bias.

## V. NON-IDEAL CURRENT-VOLTAGE CHARACTERISTICS

In the previous section the assumptions made for ideal  $p$ - $n$  junctions was discussed. However, in reality,  $p$ - $n$  junctions are from ideal and subject to a number effects in which the aforementioned assumptions do not hold. Here, two of possible departures will be discussed, as there are many possible effects that could be mentioned, but many are beyond the scope of this paper. In IV it was stated that the minority carriers are assumed to be much less than the majority carriers. First, consider the low-injection regime, where the minority carriers are much less than the majority carriers. In this case the vast majority of the potential drop occurs across the junction. The hole-concentration in the  $n$ -side is small compared to the electron concentration as pictured in the left side of fig. 7 and vice versa on the  $p$ -side. As the high-injection regime approaches, the electron concentration near the junction increases in order to maintain charge neutrality. If the concentration is increased sufficiently to reach the high-injection regime as show in the right side of fig. 7 then the potential drop across the junction is insignificant compared to the ohmic drops on both sides of the neutral regions. Another assumption made in section IV was

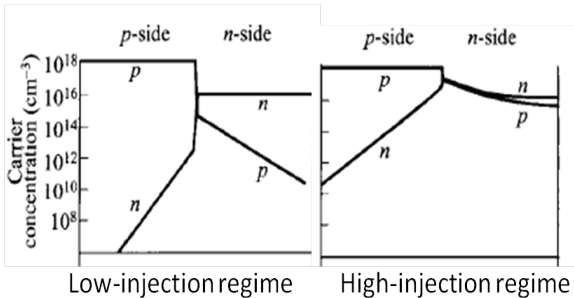


FIG. 7: Low and high-injection regimes depicted through carrier densities.

that generation and recombination does not occur in the depletion layer. However, in non-ideal cases, this does occur. Whenever the equilibrium condition of a system

is disturbed processes exist to restore the system to equilibrium. When an external bias is applied, the product  $pn$  in the transition region is different from the its equilibrium value  $n_i^2$ , since carriers are injected into ( $V_a > 0$ ) or extracted from ( $V_a < 0$ ) the transition region. To restore equilibrium, generation and recombination occurs inside the junction (recombination occurs when  $np > n_i^2$  and generation occurs when  $np < n_i^2$ ). There are two main mechanisms that can occurs in the depletion layer. First, band-to-band recombination. This occurs when an electron moves from its conduction band state into the empty valence band state associated with its hole. This band-to-band transition is also a radiative transition in direct bandgap semiconductors. A second mechanism is called Schockley-Read Hall (SRH) recombination, also known as trap-assisted recombination shown in fig. 8. This occurs when an electron falls into a trap, an energy level within the bandgap caused by some defect. Once the trap is filled it cannot accept another electron. The electron occupying the trap, in a second step, moves into an empty valence band state, thereby completing the recombination process. This can be envisioned as a two-step transition of an electron from the conduction band to the valence band or as the annihilation of the electron and the hole, which meet each other in the trap. The localized state in the gap in can absorb the difference in momentum between the carriers, and so this process is dominant in indirect bandgap semiconductors, though it can also dominate in direct bandgap material under conditions of very low carrier densities [1].

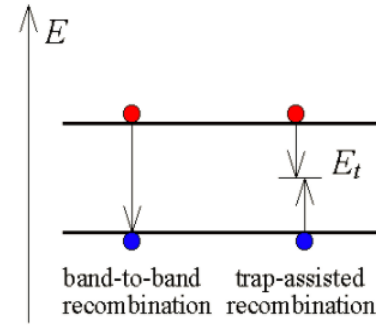


FIG. 8: Diagram of band-to-band and SRH recombination.

## VI. $p$ - $n$ JUNCTION IN 3D AND LOWER-DIMENSIONS

Thus far  $p$ - $n$  junctions in general have been discussed. However, some interesting things occur as specific dimensions are considered, namely lower-dimension devices. If one considers two 3D materials, one  $p$ -type and one  $n$ -type, then this would correspond to a 2D junction as shown in fig. 9. Likewise, 2D materials would correspond to a 1D junction. In general, it is widely assumed

that the depletion width in semiconductors is independent of dimensionality of the structure. However, this is not necessarily the case in lower-dimensional systems, such as 2D materials. For example, fig. 10 shows the result of numerical simulation of a potential profile using 1D, 2D, and 3D configurations. Note that in the 3D case the potential is essentially a delta-function potential. However, as the dimensionality decreases, this potential profile changes to a less steep potential curve. From this it implies that 3D electrostatics do not apply

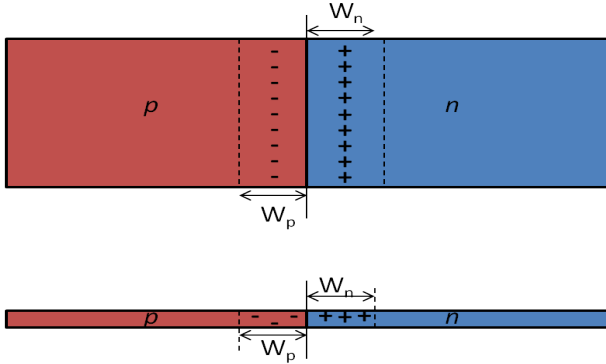


FIG. 9: Depiction of 3D and 2D junction and their corresponding depletion layer widths

to low-dimensional junctions. This high carrier densities in neutral regions of the junctions screen electric field for 3D. However, for lower dimensions this is not the case [2]. For 2D dimensional systems, the depletion width dependence is no longer similar to that in eq. 2. Rather, the depletion width becomes  $W_{2D} \propto \frac{\epsilon \Delta V}{q N t}$  where  $\Delta V$  is the combination the applied voltage and the built-in potential (similar to that of the  $\Phi_0 - V_a$  term in the 3D depletion width equation) and  $t$  corresponds to the material thickness [3]. Fig. 11 shows the depletion width

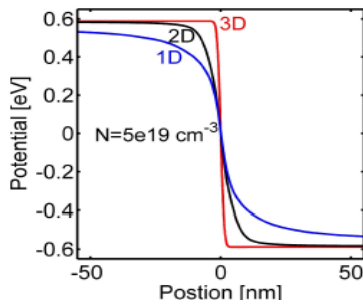


FIG. 10: Built-in potential as a function of position for 1D, 2D, and 3D.

in 1D, 2D, and 3D, as a function of thickness and doping. Notice that for large thickness the three scenarios converge to the 3D case in which there is little to no variation of the depletion width with the thickness. However, as the thickness decreases the three scenarios begin to diverge. Due to the nature of these  $p-n$  junctions in lower dimensions this opens up a new “tuning” factor, the material thickness to affect the properties of the junction. This is especially useful for new emerging materials in the 2D cases as there are many interesting properties in which the thickness dependence can be exploited.

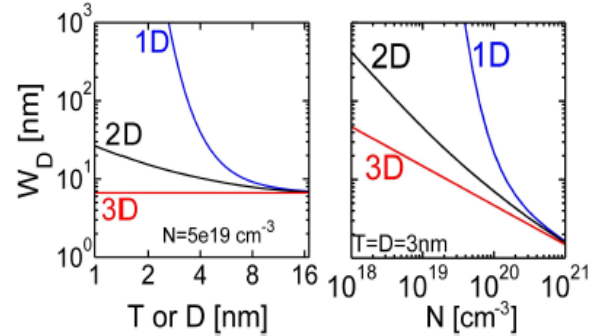


FIG. 11: Depletion width as a function of thickness (left) and carrier concentration (right) for 1D, 2D, and 3D.

## VII. CONCLUSION

The basics of  $p-n$  junctions have been discussed in the most simple context, starting from the band alignment in equilibrium and the corresponding depletion region. In addition, the non-equilibrium case has been explored and the differences from that of the equilibrium case. This leads to a discussion of the necessary assumptions made in order to fully realize the concept in a conceptual sense. However, as stated, these assumptions are not realistic in an experimental case and thus a treatment of many non-ideal parameters needs to be explored. In recent years, with the emergence of new two-dimensional materials and other lower dimensional systems, there has been a need to understand how  $p-n$  junctions behave in these regimes. Preliminary investigations show a striking difference to that of the traditional three-dimensional case and opens up new possibilities for study of the rich physics of such configurations.

[1] J.P. Colinge and C.A. Colinge. *Physics of Semiconductor Devices*. Kluwer Academic Publishers, New York City, NY, 1 edition, 2002.

[2] H. Ilatikhameneh, T. Ameen, F. Chen, H. Sahasrabudhe, G. Klimeck, and R. Rahman. Impact of Dimensionality on PN Junctions. *ArXiv e-prints*, November 2016.

- [3] H. Ilatikhameneh, T. Ameen, F. Chen, H. Sahasrabudhe, G. Klimeck, and R. Rahman. Dramatic Impact of Dimensionality on the Electrostatics of PN Junctions. *ArXiv e-prints*, April 2017.
- [4] S.M. Sze and K.K. Ng. *Physics of Semiconductor Devices*. John Wiley & Sons., 2006.